Nonequilibrium Structures in Codeposited Cr-Fe-Ni Films

E.D. Specht[a], P.D. Rack, A. Rar[a,b], G.M. Pharr[a,b], E.P. George[a,b], and H. Hong[c],
[a]Metals and Ceramics Division, Oak Ridge National Laboratory, Oak Ridge, Tennessee, 37831-6118, USA
[b]Department of Materials Science and Engineering, University of Tennessee, Knoxville, Tennessee, 37996, USA
[c]Frederick Seitz Materials Research Laboratory, University of Illinois at Urbana-Champaign, Urbana, Illinois, 61801, USA

ABSTRACT

Ternary libraries are prepared by codeposition of Cr, Fe, and Ni on single-crystal Si and Al_2O_3 (sapphire) substrates at ~100°C. The varying proximity to the three metal sources produces a spread of compositions in the films, which are analyzed both as-deposited and after annealing in vacuum for 2 h at 500°C. Structural maps are produced using synchrotron radiation and simultaneous detection of 2D diffraction patterns and x-ray fluorescence spectra. Four phases are identified in the as-deposited films. Three phases occur in equilibrium: bcc (α), fcc (γ), and intermetallic (σ). The fourth phase does not correspond to any equilibrium phase in the Cr-Fe-Ni system; it is tentatively identified as isomorphic to the α–Mn (A12) structure. After annealing, the nonequilibrium phase is no longer observed, but the occurrence of the three equilibrium phases is still far from the equilibrium phase boundaries. The particle size measured by x rays is small (9-15 nm), suggesting that higher annealing temperatures are required for the growth of equilibrium phases.

INTRODUCTION

Film growth by physical vapor deposition presents opportunities to produce material far from thermal equilibrium; material is deposited with high energy, cooling rapidly on contact with the substrate. A wide variety of nonequilibrium phases have been reported both in the Fe-Cr binary system [1,2] and the Fe-Cr-Ni ternary system [3]. While the binary system has been studied over a wide range of compositions, the ternary system has been studied only at isolated compositions. Because Fe-Cr-Ni is of broad interest for both structural and magnetic properties and applications, we are undertaking a comprehensive survey of the structural properties of sputtered films, looking for metastable phases and their behavior on annealing. Combinatorial analysis is a powerful tool to search these materials for nonequilibrium structures. Ternary libraries are prepared by codepositing material from three sources; the composition of the film will vary depending on the relative proximity of the sources. Synchrotron radiation is used as a tool for rapidly identifying the structures initially formed and for studying how they change on annealing. This analysis technique has recently been demonstrated using the equilibrium phases of the Cr-Fe-Ni system, formed by sequential deposition followed by interdiffusion [4].

EXPERIMENTAL DETAILS

Four samples of thin films alloys were deposited using an RF magnetron sputtering

Table I. Description of samples. NF: not found, or too weak to measure.

Sample ID	Substrate		annealing		x-ray crystallite size (nm)			
	Orientation	Diameter (mm)	Temp. (°C)	Time (h)	bcc	fcc	σ	α-Mn
A	Al_2O_3 $(11\bar{2}0)$	50	500	2	12	15	19	NF
B	Al_2O_3 $(1\bar{1}02)$	50	500	2	11	9	16	NF
C	Al_2O_3 $(11\bar{2}0)$	50	none		9	15	16	>30
D	Si (100)	100	none		8	NF	14	>29

system. Substrate compositions, orientations, and dimensions are listed in Table I. Fig. 1 shows the 3-source assembly illustrating the source positions relative to the substrate. The sputtering system has three 2” sources that were simultaneously sputtered onto a fixed substrate. Each source has a 2” tall shield around each target to minimize the possible cross-contamination from source to source. The iron and nickel sources were oriented 180° apart in the chamber and the chromium target was oriented 90° from both the iron and nickel targets. All the target centers are 16.5 cm from the 4” substrate holder center and are tilted at 32° relative to the substrate normal to create a composition gradient across the substrate. Incidental heating from the sputter sources raised the sample temperature to ~100°C during deposition.

For each deposition, the base pressure was nominally $7x10^{-7}$ Torr and the processing pressure was 10^{-3} Torr argon. The sputtering powers for the targets were Fe-160W, Cr-60W, Ni-60W and each film was deposited for three hours. The sputtering power controls the deposition rate and these powers were arrived at by experimentally measuring the deposition rate of each material and estimating the appropriate sputtering powers necessary to yield the σ phase field near the Fe-Ni side of the ternary diagram. Film thickness was ~2μm. Selected samples were annealed in vacuum as described in Table I. Films on Si substrates delaminated during annealing and were not studied.

Diffraction and fluorescence data were collected using the bending magnet beamline X33-BM at the Advanced Photon Source. A double-crystal Si(111) monochromator was used to select 12 keV x rays, which were sagitally focused by the monochromator and meridionally focused by a pair of mirrors, which also provide harmonic rejection. The focused beam size was 1.0 x 0.25 mm^2, providing a 1.0 x 1.0 mm^2 footprint on the sample when incident at a 15° glancing angle. The sample was mapped by rastering in 1 mm steps. Data were collected for 2 s at each point.

Fluorescence spectra were acquired using a Si drift detector with resolution of 165 eV at 6.4 keV. The detector views the sample at a 15° glancing angle, the angle of the incident x rays. A typical energy spectrum is shown in Fig. 2. The integrated counts in the Cr, Fe, and Ni K_α and K_β lines were measured by least-squares fitting to Gaussian lineshapes. Composition was calculated from the ratios of these count rates as described previously [4]. Because the sample thickness is not constant, we apply the thick film limit in calculating composition; because the data are collected at glancing incidence, this introduces a negligible error. A

Fig 1. The 3-source configuration for the combinatorial sputter deposition process.

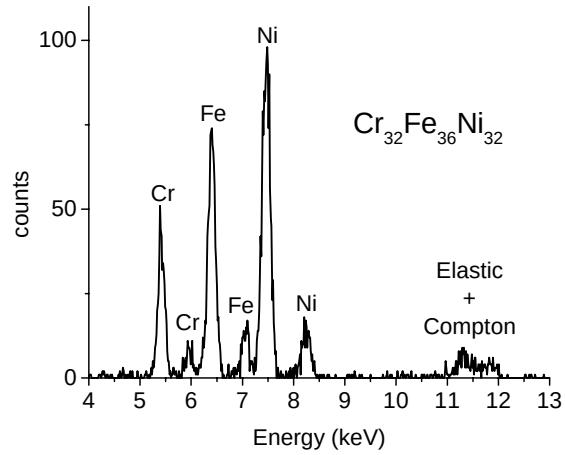

Fig. 2. Fluorescence spectrum from sample A with Kα and Kβ emission peaks labeled.

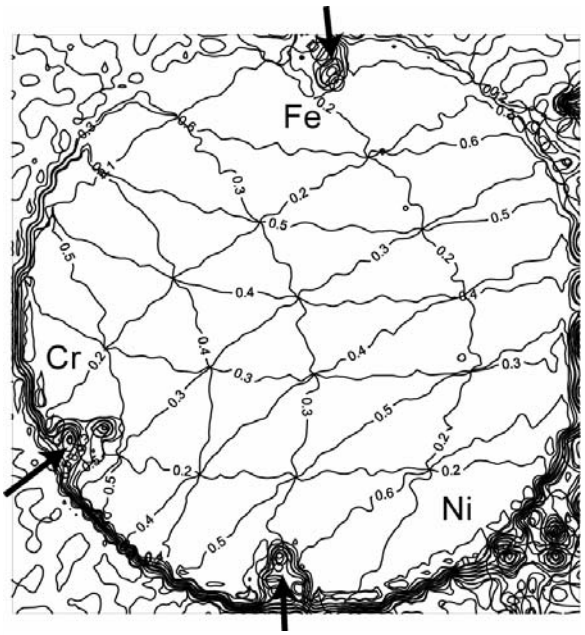

Fig. 3. Composition map of sample D, with contours of constant Cr, Fe, and Ni composition. Elemental labels indicate area of maximum concentration, and can be used to identify the contour lines. Arrows indicate areas masked by the sample holder. Contours beyond the perimeter of the circular wafer have no significance.

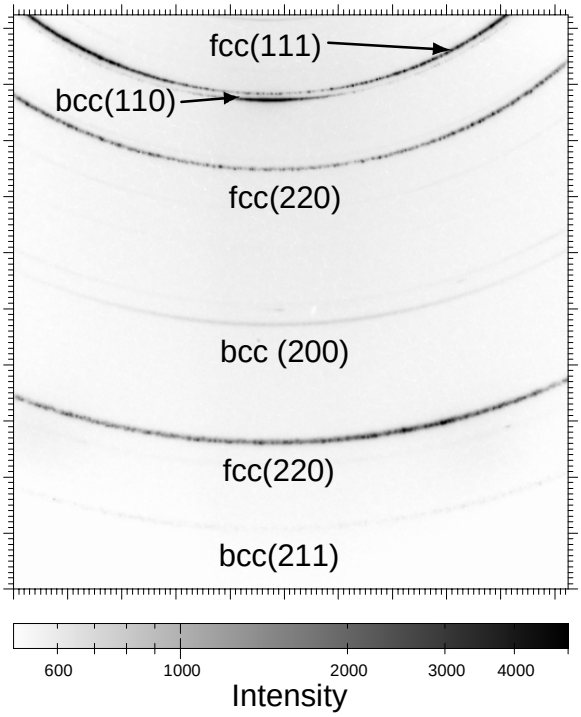

Fig. 4. Diffraction pattern from sample A. Labeled are an epitaxial bcc phase and a weakly textured fcc phase.

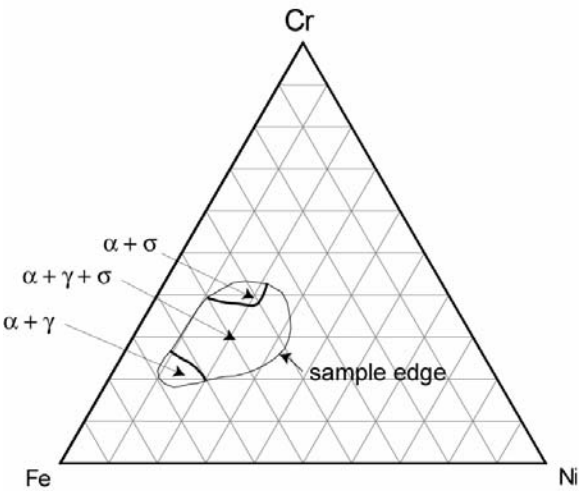

Fig. 5. Phase diagram, sample A.

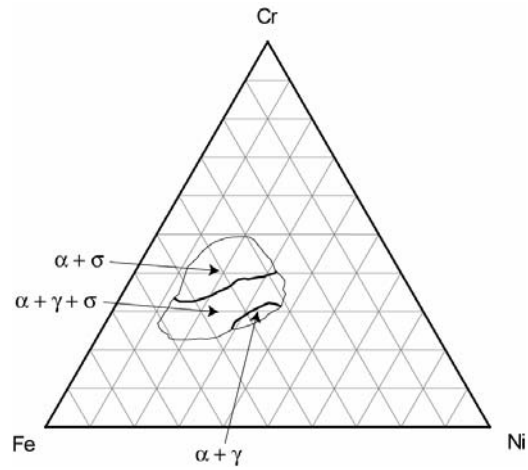

Fig. 6. Phase diagram, sample B

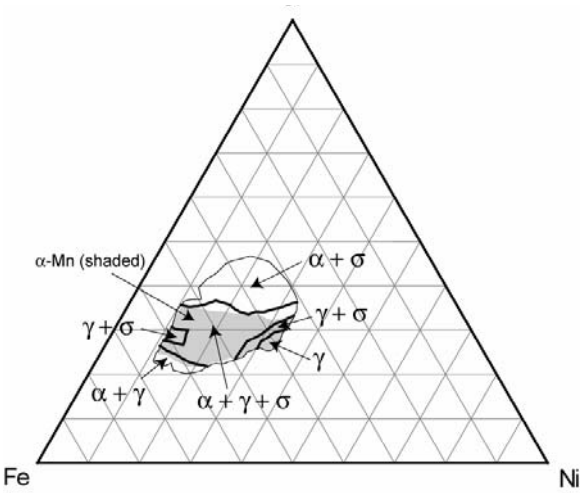

Fig. 7. Phase diagram, sample C

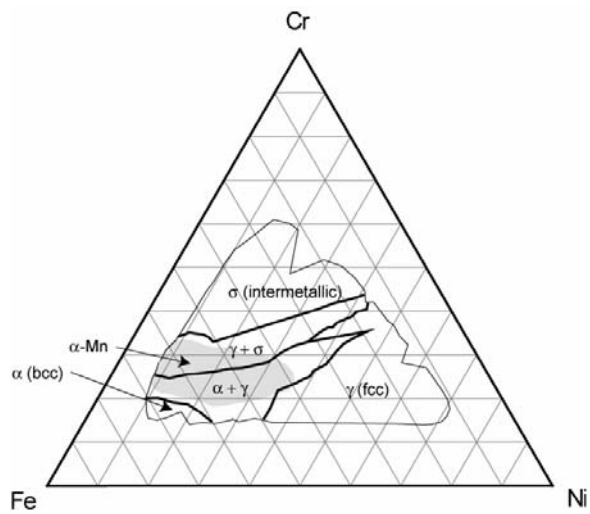

Fig. 8. Phase diagram, sample D

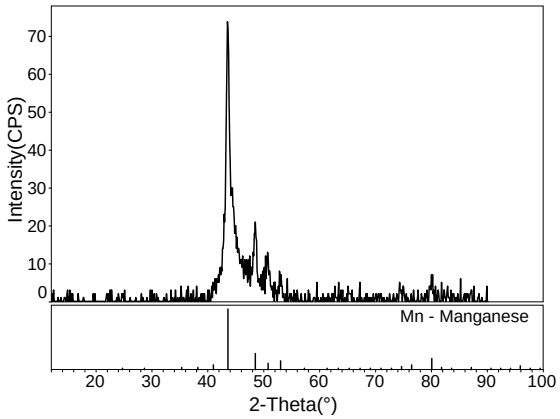

Fig. 9. Diffraction pattern for α-Mn structure, using a laboratory Cu Kα source at a 70° tilt.

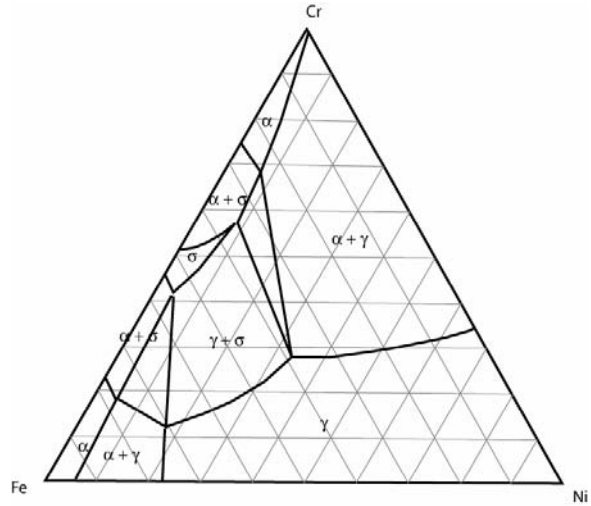

Fig. 10. Isothermal phase diagram section at 560°C

typical composition map is shown in Fig. 3.

Diffraction patterns were taken using a 1024 x 1024 pixel CCD detector. A typical diffraction pattern is shown in Fig. 4. Phases were identified as described earlier [4]. Phase diagrams are shown in Figs. 5-8. An unexpected phase appears, in addition to the expected α (bcc), γ (fcc) and σ (intermetallic) phases [5]. Because it does not appear as a single phase, and because the quality of the diffraction patterns is limited by the small grain size of the sample (as discussed below), we cannot positively identify this phase. By tilting the sample, we are able to minimize scattering from other phases, and the remaining pattern is consistent with the α-Mn (A12) structure, as shown in Fig. 9. α-Mn is cubic with a lattice parameter a_0=0.8911 nm [6]; we observe a_0=0.880 nm.

The diffraction patterns show broadening beyond instrumental resolution. Peak broadening is frequently caused by two factors. Microstrain, a distribution Δd of plane spacings d among the diffracting crystallites, produces peak broadening $\Delta 2\theta = 2\tan\theta\ \Delta d / d$. Small particles of size L produce broadening $\Delta 2\theta = 0.94\lambda/(L\cos\theta)$. Because these two effects have different θ dependence, they can be distinguished by comparing the width of two reflections [7]. We find that the ratio of widths of the fcc(220) and fcc(111) reflections is consistent with small particle size rather than microstrain. Assuming that the bcc phase is broadened by particle size as well, we calculate particle sizes as shown in Table I. The α-Mn peak widths are limited by instrumental resolution, so we have only a lower bound to the particle size of this phase.

DISCUSSION

The samples which have not been heat treated (Figs. 7, 8) are clearly not in equilibrium. Firstly, the phase boundaries do not correspond to any known isothermal section of Cr-Fe-Ni. Secondly, the α-Mn structure appears, which is not a known equilibrium phase in the Cr-Fe-Ni system. This structure has been reported to occur in $Fe_{82.5}Cr_{17.5}$ alloys grown by cosputter deposition with ion assistance during deposition [2]. Thirdly, the coexistence of four phases is observed in sample C over a two-dimensional field, while the Gibbs phase rule allows four phases to coexist only along a line [8, p. 7-11]. Combinatorial analysis of composition-spread thin film samples may prove to be a powerful tool for the discovery of nonequilibrium phases.

While the four-phase field and the α-Mn structure disappear after annealing (Figs. 5, 6), the phase boundaries are still far from the published equilibrium values near the annealing temperature (Fig. 10). The annealing time and temperature are apparently too low for the sample to reach equilibrium. Equilibration by longer annealing times at higher temperatures is needed as an important confirmation that the samples are not affected by contamination or reaction with substrate or atmosphere.

No significant grain growth is observed on annealing (as measured by x-ray crystallite size, Table I), supporting the conclusion that time and temperature are insufficient for equilibration. The crystallite size for the α-Mn phase is much larger than that of the others, suggesting that it is formed by a recrystallization from the other phases. The large growth stress which can occur during low temperature sputtering is a possible cause of the transformation to the nonequilibrium α-Mn phase.

There are pronounced differences between the two annealed samples, despite similar

processing. Sample A, grown on $Al_2O_3(11\bar{2}0)$, has a more pronounced epitaxy, with bcc (110) and fcc(200) planes growing nearly parallel to the sample surface. Sample B, grown on Al_2O_3 $(1\bar{1}02)$, grows with a more random texture and has a larger grain size. Both effects suggest that the substrate for sample A has a more atomically smooth surface.

CONCLUSIONS

Cr-Fe-Ni films sputtered at low temperatures show nonequilibrium structures, including a phase tentatively identified as the α-Mn structure. This metastable phase disappears on annealing (500°C, 2 h), but the films still do not approach the equilibrium phase diagram, nor does significant grain growth occur. In future work, we will determine the temperatures at which the metastable structure disappears and the phase boundaries approach their equilibrium values.

ACKNOWLEDGMENTS

Work sponsored by the U.S. Department of Energy, Division of Materials Sciences and Office of Industrial Technologies, Industrial Materials for the Future Program, under grant number DE-FC07-02ID14251. Oak Ridge National Laboratory (ORNL) is operated by UT-Battelle, LLC, for the U.S. Department of Energy under contract DE-AC05-00OR22725. The UNICAT facility at the Advanced Photon Source (APS) is supported by the Univ of Illinois at Urbana-Champaign, Materials Research Laboratory (U.S. DOE, the State of Illinois-IBHE-HECA, and the NSF), the Oak Ridge National Laboratory (U.S. DOE under contract with UT-Battelle LLC), the National Institute of Standards and Technology (U.S. Department of Commerce) and UOP LLC. The APS is supported by the U.S. DOE, Basic Energy Sciences, Office of Science under contract No. W-31-109-ENG-38.

REFERENCES

[1] A.A. Levin, D.C. Meyer, A. Tselev, A. Gorbunov, W. Pompe, and P. Paufler, J. Alloys Compd. **334**, 159-166 (2002).

[2] M.C. Simmonds, R.C. Newman, S. Fujimoto, and J.S. Colligon, Thin Solid Films **279**, 4-6 (1996).

[3] E. Kuzmann, G. Principi, C. Tosello, K. Havancsák, S. Stichleutener, I. Geröcs, Z. Homannay, and A. Vértes, Nucl. Instrum. Methods Phys. Res., Sect. B **183**, 425-431 (2001).

[4] E. D. Specht, A. Rar, G.M. Pharr, E.P. George, P. Zschack, H. Hong, and J. Ilavsky, J. Mater. Res. **10**, 2522-2527 (2003).

[5] Y.-Y. Chuang and Y.Y. Chang, Metall. Trans. A **18**, 733-745 (1987).

[6] J.A. Oberteuffer and J.A. Ibers, Acta Crystallogr., Sect. B: Struct. Sci. **26**, 1499-1504 (1970).

[7] G.K. Williamson and W.H. Hall, Acta Met. **1**, 22-31 (1953).

[8] F.E.W. Wetmore and D.J. LeRoy, *Principles of Phase Equilibria*. (McGraw-Hill, New York, 1951).